

AD-A205 193

ELECTRON DENSITY PROFILES AND PLASMA DRIFT MEASUREMENTS
WITH DIGITAL IONOSONDES (U) LOWELL UNIV MA CENTER FOR
ATMOSPHERIC RESEARCH B H REINISCH ET AL. SEP 88
ULRF-442 CAR AFGL-TR-88-0233

1/1

UNCLASSIFIED

F/G 4/1

NL

1.0
1.1
1.25
1.4
1.6
1.8
2.0
2.2
2.5
2.8
3.2
3.6
4.0
4.5
5.0
5.6
6.3
7.1
8.0
9.0
10.0
11.2
12.5
14.0
16.0
18.0
20.0
22.4
25.0
28.0
31.5
36.0
40.0
45.0
50.0
56.0
63.0
71.0
80.0
90.0
100.0

AD-A285 193

UNCLASSIFIED

REPORT DOCUMENTATION PAGE

Form Approved
GSA GEN. REG. NO. 27

| | | | |
|---|--|---|--|
| 1. REPORT NUMBER AFGL-TR-88-0233 | | 2. REPORT TYPE N/A | |
| 3. REPORT CATEGORY N/A | | 4. REPORTING ORGANIZATION REPORT NUMBER AFGL-TR-88-0233 | |
| 5. NAME OF REPORTING ORGANIZATION University of Lowell Center for Atmospheric Research | | 6. NAME OF REPORTING ORGANIZATION Air Force Geophysics Laboratory | |
| 7. ADDRESS (City, State, and ZIP Code) 450 Aikman Street Lowell, Massachusetts 01854 | | 8. ADDRESS (City, State, and ZIP Code) AFGL/LIS Hanscom AFB, MA 01731 | |
| 9. NAME OF FUNDING/SPONSORING ORGANIZATION Air Force Geophysics Laboratory | | 10. FUNDING INSTRUMENT IDENTIFICATION NUMBER F19628-86-K-0036 | |
| 11. ADDRESS (City, State, and ZIP Code) AFGL/LIS Hanscom AFB, MA 01731 | | 12. NAME OF FUNDING AGENCY PROJECT NO. 4643 TASK NO. 06 WORK UNIT ACCESSION NO. AJ | |
| 13. TITLE (Include Security Classification) Electron Density Profiles and Plasma Drift Measurements with Digital Ionosondes | | | |
| 14. AUTHOR(S) Rodo W. Reinkens, Jürgen Buchen, * Robert R. Gnancho, Klaus Bibl, Gary E. Balaz, Evans Harris, ** Lee P. McManus*** | | | |
| 15. TYPE OF REPORT Scientific Report No. 2 | | 16. DATE OF REPORT (Year, Month, Day) 1988, September | |
| 17. DATE OF REPORT (Year, Month, Day) 1988, July '87 to June '88 | | 18. PAGE COUNT 32 | |
| 19. REPORTING ORGANIZATION AFGL/LIS, Hanscom AFB, MA 01731, **Research Institute of Radiowave Propagation, P.O. Box 138, Kluksburg, Roman, PRC, ***Andrew Antennas, Innovation House, Technology Park, The Levels, S.A. 5095, Australia | | | |
| 20. SUBJECT TERMS (Include Security Classification) Ionospheric; Electron Density Profiles; Digital Ionosonde; Ionospheric Drift; Tilt and Roughness. | | | |
| 21. ABSTRACT (Include Security Classification) Knowledge of the three dimensional electron density distribution and the plasma drift in the earth's ionosphere is needed for the radio communication engineer and the geophysicist. The combination of global models, e.g. the International Reference Ionosphere (IRI), modern digital ionosondes, and relatively powerful micro-computers provide the capabilities to overcome the limitations that have heretofore prevented real time ionospheric specification and improved forecasting techniques. The developing network of digital ionosondes provides an improved ionogram data set. The cumbersome evaluation of electron density profiles (EDP), from the ionograms, has been eased with automatic ionogram scaling and related micro-computer based algorithms for calculating EDPs. The purpose of this Scientific Report is to summarize the evolving network of digital ionosondes based on the Sigasende 234 technology and to present techniques that have been developed for calculating electron density profiles and determining the drift velocities. (Continued) | | | |
| 22. DISTRIBUTION STATEMENT OF ABSTRACT UNCLASSIFIED | | 23. DISTRIBUTION STATEMENT OF ABSTRACT UNCLASSIFIED | |
| 24. NAME OF REPORTING ORGANIZATION Johanna E. Henshaw | | 25. NAME OF REPORTING ORGANIZATION AFGL/LIS | |

Form 100, 100-10

Previous editions are obsolete.

SECURITY CLASSIFICATION OF THIS PAGE

UNCLASSIFIED

UNCLASSIFIED

19. ABSTRACT (Continued)

In addition, examples are presented to illustrate related data summaries that can be developed and tailored to the needs of the communication or radar system manager and to the needs of the geophysical research in basic and applied research in solar-terrestrial physics. *key words: → to field 18*

UNCLASSIFIED

TABLE OF CONTENTS

| | Page |
|--|------|
| FOREWORD | 1 |
| MULTISTATION/MULTIPARAMETER OBSERVATIONS WITH A NETWORK OF DIGITAL IONOSONDES | 5 |
| REAL TIME ELECTRON DENSITY PROFILES FROM IONOGRAMS | 14 |
| LAY-FUNCTIONS FOR F2 PROFILES | 24 |



| | |
|--------------------|-------------------------------------|
| Accession For | |
| NTIS CR&I | <input checked="" type="checkbox"/> |
| DTIC TAB | <input type="checkbox"/> |
| Unannounced | <input type="checkbox"/> |
| Justification | |
| By | |
| Distribution/ | |
| Availability Codes | |
| Dist | Avail and/or Special |
| A-1 | |

FOREWORD

Within several years, a worldwide network of approximately 40 digital ionosondes will be operating to further understanding of solar-terrestrial and radio physics. The digital ionosondes possess capabilities to provide data bases that heretofore were limited to instruments requiring a significant capital investment (e.g. incoherent scatter radar) or were labor intensive to obtain (e.g. real-height analyses).

With the maturation of the Digisonde hardware, there has been associated analytical work to develop automatic, micro-computer based algorithms that will provide reliable data bases of the aforementioned types.

The University of Lowell Center for Atmospheric Research, with cooperation and support from the Air Force Geophysics Laboratory recently contributed three papers that document the planned digital ionosonde network and the approaches and results of the associated analytical investigations.

The first paper summarizes the global Digisonde 256 network, the ionogram and drift operating modes and the resulting data. The drift mode of operation, in addition to determining the mean ionospheric motion within the instrument's field-of-view, provides high resolution Doppler spectra of the signals obtained from seven spaced receiving antennas. These data can be used to determine ionospheric tilt and roughness. Data editing and processing programs have been developed to present, on a single page, ionospheric characteristics and ionogram surveys. These examples serve as a base for defining data handling and archival formats that can result from these improved, contemporary data sets. The

examples are shown to illustrate how the resulting data may be summarized and presented to benefit the radio communications engineer and the geophysicist.

The second paper summarizes the techniques developed by the University of Lowell Center for Atmospheric Research (ULCAR) group to determine the true height electron density profile from the virtual height ionogram trace. The ULCAR technique is based on a sum of the shifted Chebyshev polynomials that represents the true height for each ionospheric layer. The methods for determining the ionospheric profile starting height and the conditions for joining the layers are discussed in this paper. A comparison is made of the ULCAR and POLAN (Chapman profile shape) profiling methods. An analysis of 172 ionograms reveals an average height difference of -2.0 kilometers and a mean peak height difference of +7.6km. Given electron density profiles, a comparison is made of the Dudney ionospheric model heights of the F2 layer as a function of the ratio of foF2 to foE. It was found that the Dudney model yields systematically high height values for daytime and low height values for nighttime. It is suggested that these systematic differences may result from the model's neglect of underlying ionization or a variation of the F2 region scale height with altitude. The modern ionosonde produces important data for understanding ionospheric phenomena and for the development of improved ionospheric models. The utility of these modern data is not limited by the storage media, and new opportunities are opening for tailored data presentation, analysis and archival consistent with the needs of the application and research communities.

The third paper discusses an alternative representation of the F2 region electron density profile. The ULCAR Chebyshev polynomial requires five coefficients plus the beginning and ending frequencies of the layer. In the POLAN single-polynomial mode, 11 parameters are needed to represent the F2 electron density profile. The LAY function, defined by four parameters [f_oF2 , H_{max} (peak height), HX (height parameter) and SC (scale parameter)], may lend itself to improved real time processing. Three thousand electron density profiles calculated from the POLAN fourth order polynomial expansion were compared to the profiles determined using the LAY function. The comparison shows that for most of the time the LAY functions, with five kilometer maximum error, represent the F2 layer down to $f = f_oE$ or f_oF1 during the day and to the first scaled ionogram frequency during the night. It was also found that the LAY function parameters (HX/H_{max} and SC) have fairly small diurnal variations in their median values. This study could be expanded to represent the entire electron density profile as a linear combination of LAY functions and to investigate the behavior of the associated LAY parameters.

This scientific report includes the recent papers mentioned above:

Reinisch, B. W., J. Buchau, K. Bibl and G. S. Sales, "Multistation/Multiparameter Observations with a Network of Digital Ionosondes," invited paper presented to the Electromagnetic Wave Propagation Panel, North Atlantic Treaty Organization, Advisory Group for Aerospace Research and Development, Munich, Federal Republic of Germany, May 1988. Proceedings forthcoming.

Reinisch, B. W., R. R. Gamache, H. Xueqin and L. F. McNamara, "Real Time Electron Density Profiles from Ionograms," Advances in Space Research. Ionospheric Informatics, 8, 4, (4)63-(4)72, 1988.

Boesy, L., R. R. Gamache and B. W. Reinisch, "LAY-Functions for F2 Profiles," Advances in Space Research. Ionospheric Informatics, 8, 4, (4)201-(4)204.

1

B. M. Reinisch, (1) J. Bucher, (2) K. Eibl (1) and G. S. Sales (1)

(1) University of Lowell Center for Atmospheric Research, Lowell, MA 01854, U.S.A.

(2) Air Force Geophysics Laboratory, Hanscom AFB, MA 01921, U.S.A.

Summary

The global network of modern ionosondes generates a data set of ionospheric characteristics that can serve as test bed for the developing ionospheric models. Remote access to each station makes it possible to use real time data for project planning and radio communication tasks. New ionospheric parameters like ionospheric roughness, tilt angles and drift are now available for each Digisonde location.

1. Introduction

A new generation of modern ionosondes is now being deployed world-wide. By the end of 1990, a network of some forty of these ionosondes (Heinsch, 1988) will provide a consistent data set of ionospheric parameters that are automatically scaled in real time. The automated stations output the standard ionospheric parameters, the f^oF_2 traces with amplitudes and Doppler frequencies, and the electron density profiles. All these data can be remotely accessed by telephone links, and they are, in general, archived on half-inch magnetic tape.

New measuring techniques make it possible to determine ionospheric structure and dynamics in a more or less routine way. After completion of an ionogram, the sounder measures ionospheric drift and structure using high resolution Doppler shift and incidence angle observations. High latitude drift observations monitor the polar cap convection pattern, and first results from Millstone Hill (42.6°N, 71.3°W) show that this pattern can also control the drift at this mid-latitude location. F-layer tilts, measured at mid-latitude, show typical tilt angles of 2 to 5°; values of 15° are observed occasionally. Observations of the smoothness of the mid-latitude F-layer, as defined by the inverse of the size of the reflection area, show a characteristic day/night variation. During the day the echoes arrive within a small angular cone of $\theta < 5^\circ$ (smooth ionosphere), while this angle increases to some 30° at night (rough ionosphere).

2. Digisound Network

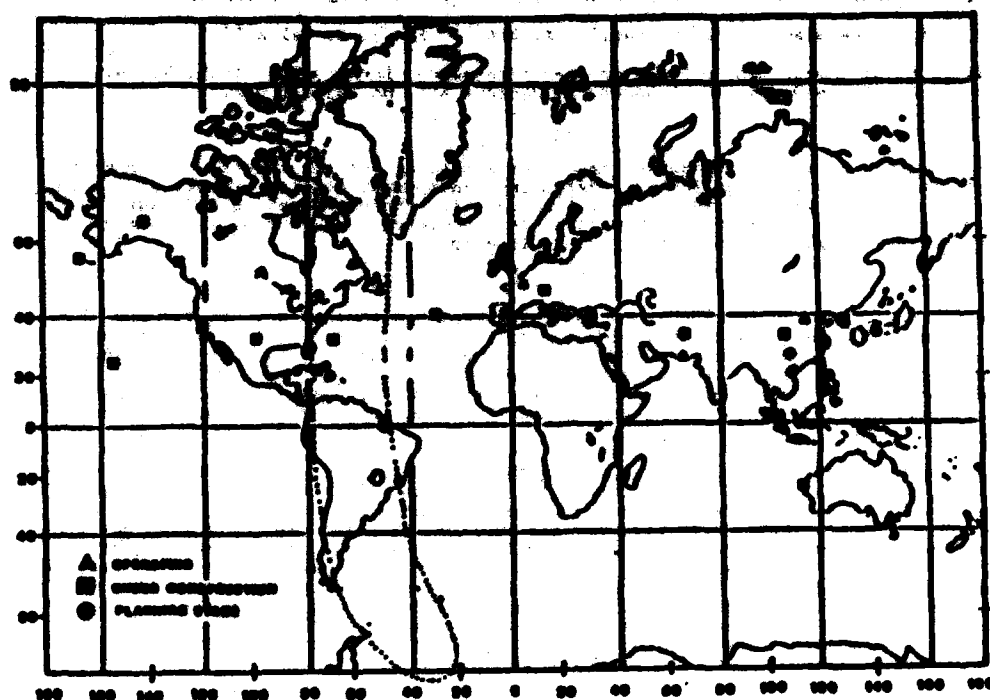
[illegible]

There are currently 22 Digisonde 254 systems (Table 1) in operation or are close to being installed. The global station distribution, as shown in Figure 1, is very uneven, the majority of sites lying in the northern hemisphere, and there are no equatorial stations. Nevertheless this network provides an extensive data base of ionospheric parameters in digital form, making it easy to process and analyze the data in terms of average diurnal variations, storms, and irregularities. This data base will be invaluable for the testing of global ionosphere models.

The sealed isogram parameters and/or the raw isograms can be remotely accessed via voice grade telephones line operating at 1200 or 2400 baud. Currently only the U.S. Global Air Weather Service is networking in a real time mode by polling all their 6816meters and centrally collecting the isomeric parameters as soon as an isogram scan and the 20 to 30 second ARTIST processing is completed. In general, all stations record the raw isograms and the autocoded data on half-inch magnetic tape (1200 bpi).

By adding transmit antennas for oblique transmissions to the stations the Digiscanner can be used to record oblique digital ionograms (Rishbeth et al., 1984; Ahmed et al., 1986). A project is underway to automate both operation and sorting for oblique ionograms, thus adding more sampling points to the digital data set.

Total 1



GLOBAL DIGISONDE 256 NETWORK

Figure 1

2. Ionospheric Data

The Digisonde 256 has three basic modes of operation: (1) vertical incidence ionograms, (2) drift observations, and (3) oblique incidence (bistatic) ionograms. Since the third mode is not yet fully automated and the necessary processing software is not yet developed, we limit the discussion to modes 1 and 2.

2.1 Ionogram Characteristics

The Digisonde scales the ionogram within 20 to 30 seconds after completion of the ionogram scan using the ARTIST routine (Painchaud and Huang, 1988). Figure 2 is an example of a typical on-line printout from the University of Lowell station at Millstone Hill in Westford, MA (42.6°N, 71.0°W geom.). The small numbers using optically weighted fast Fourier transforms (Painchaud et al., 1983) give the amplitudes in multiples of 1 dB for the vertical incidence echoes with ordinary polarization, the E indicates extraordinary polarization, and the arrows point to the direction from where oblique echoes are received. The arrows composing the E traces at 130 km all point to the north-east. The oblique F echoes between 0.5 and 6.0 MHz come from the south and southwest. ARTIST finds the leading edge of the overhead echo traces for the E and F layers. The automated $h'(f)$ traces, marked by the letters E and F, are superimposed on the raw ionogram, thus providing a means of checking the ARTIST performance. The letter F is used for presenting the calculated true height profile. For each layer, E, F1 and F2, the profile is given in terms of a modified sum of Chebyshev polynomials (Gonzalez et al., 1988). The coefficients of the Chebyshev polynomials are stored on magnetic tape and transmitted to the data center via telemetry links. ARTIST scales the following ionogram parameters: f_{oF2} , f_{oF1} , f_{oE} , f_{min} , $MUF(3000)$, $M3000$, $h'F$, $h'F1$, $h'E$ and $h'Es$. The frequency spread for both E and F is determined, and also the average range spread (listed as fE , fF , QE and QF in Figure 2). The virtual height traces $h'(f)E$ and $h'(f)F$ are recorded together with the measured echo amplitudes and Doppler frequencies.

Is the quality of the automated data adequate for the high frequency radio communication and radar engineers, and for the ionospheric modelers? Recent comparisons of ARTIST scalings for f_{oF2} and $MUF(3000)$ with manual readings by experienced ionogram scalars (Gilbert and Smith, 1988) show that ARTIST provides acceptable values for about 93% of the time at a mid-latitude station. For 87% of the analyzed ionograms, f_{oF2} was determined within 0.5 MHz. This is somewhat better than the 87% (Painchaud and Huang, 1988) found for the auroral station at Goose Bay (64.6°N geom.).

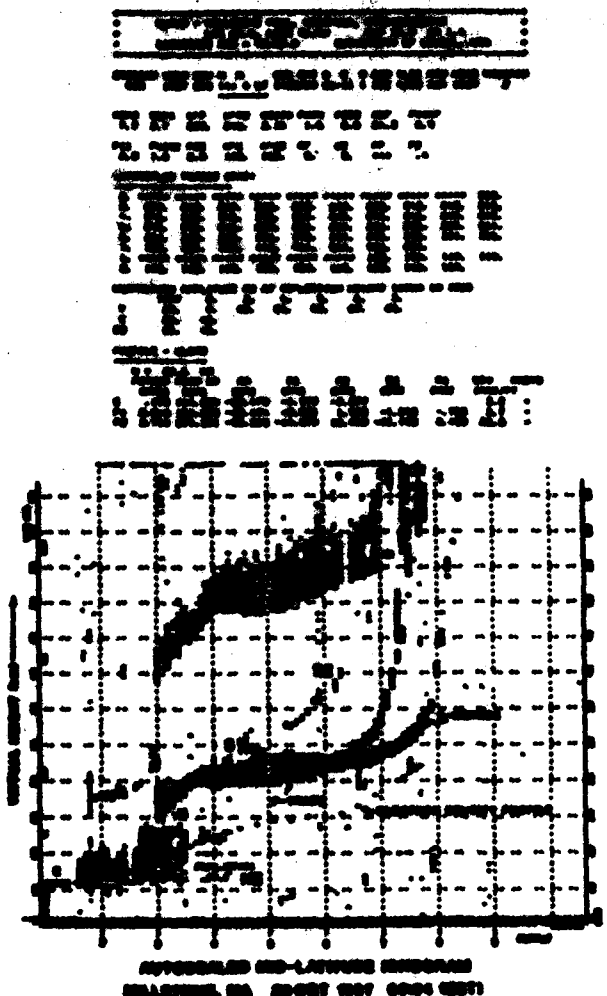


Figure 2

The WLCAR group has recently developed the ARTIST Data Editing Program (ADEP) to establish a quality control for the ARTIST data. Inconsistent values are automatically detected, the raw ionogram together with the ARTIST traces are displayed on a computer display screen, and an operator can make the required corrections. The electron density profiles are updated automatically. The edited ARTIST data are then recorded on a 1.2 Mbyte floppy disk which can store the characteristics for about 1,700 ionograms. This floppy disk will be the form in which the data of the WLCAR station will be published, containing much more information than is normally published by ionospheric stations. Besides the standard ionospheric parameters the disk contains the echo traces, i.e. $h'(f)$, the echo amplitudes and Doppler frequencies and the coefficients for the calculation of the electron density profiles.

A companion program to ADEP prints frequency plots and electron density contours, as shown in Figure 2, displaying the data for 10 October 1987 at Millstone. f_oF_2 , f_oE_s , f_{u1} and f_{u2} are plotted in the top panel. The extent of the frequency spread of the

F trace is indicated on the foF2 curve. The lower half of the figure shows the height variations for given electron densities (plotted as plasma frequency contours in 0.1 MHz increments); the top curve is h'pF2. Local midnight and noon are marked by M and N, and sunrise and sunset is marked by an F and an E for the F and E region, respectively. It is proposed that this display become the standard presentation for the data from the Digiscand network. For specific case studies it may be useful to review the original ionograms. The ionogram survey (Figure 4) displays the 96 quarter hour ionograms for one day on a single page. Only overhead echoes with ordinary polarization are printed, oblique and X polarization echoes are deleted.

3.2 Drift Mode Data

In the drift mode, the Digiscand determines high resolution Doppler spectra for each of the signals received on seven spaced receiving antennas (Reinisch et al., 1967, Buchau et al., 1967). The incidence angle of each spectral signal component is calculated from the seven respective phases, resulting in a skymap that shows the location of the simultaneously existing reflection points (sources) and their respective Doppler frequencies. Tight clustering of the sources indicates a smooth ionosphere, wide spread a rough ionosphere. We defined a roughness index RI that is proportional to the angular extent of the source region. Figure 5 shows this index for Erie, CO, during a disturbed period in March and a quiet period in April. The solar zenith angle is plotted on top of the figure. The roughness index of 2 at noon indicates an angular size of the reflection area of about 10°, while RI = 12 at night during the disturbed period indicates 60°. This pattern of smooth daytime and rough nighttime contours was seen on all the Colorado data and also on data from the subauroral station at Argentina, Newfoundland (Figure 6). The night RI increases with increasing magnetic activity as illustrated in Figures 5 and 6.

This center of gravity of the source locations defines the tilt vector consisting of a tilt angle, measured from the overhead position, and tilt direction, measured clockwise from true north. The diurnal variation of these two parameters for Erie, CO is shown in Figure 7 for 5/6 March 1968. These tilt parameters are well defined only when the ionospheric roughness is small. There is a large uncertainty in defining the tilt parameters when the sources are spread over the sky. Figure 7 indicates a consistent southward tilt increasing from 2° to 3° during the daytime. Large angles of up to 10° are occasionally observed.

When the sources are sufficiently spread the three-dimensional drift velocity vector which best reproduces the observed Doppler frequencies (Dossis, 1963) is calculated. In general, we assume a uniform plasma velocity over the entire skymap (zenith angle $\theta < 90^\circ$). Routine observations in the polar cap and the auroral regions (Buchau et al., 1967) show the predominantly antisunward plasma convection for long periods of time.

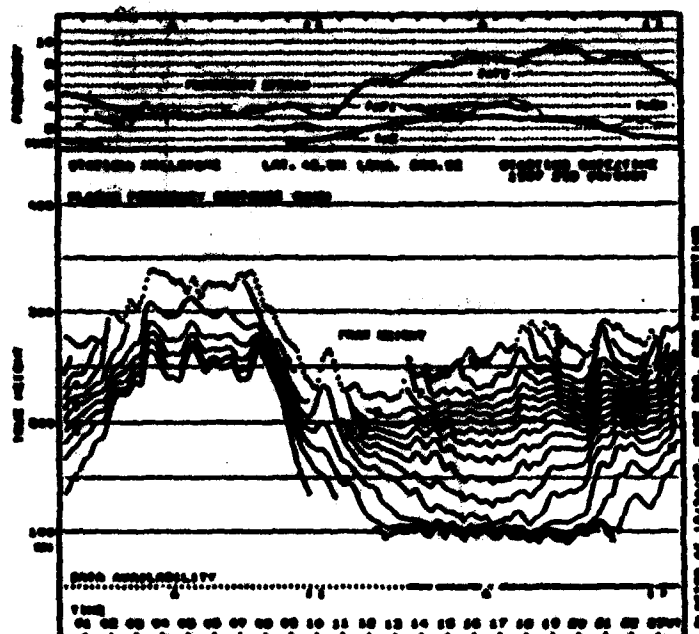
The F region drift in the central polar cap (Qanaq, Greenland, 87.6°N CBL) is shown for five consecutive days, October 18 to 22, 1967 in Figure 8. Direction and magnitude of the horizontal drift vector are plotted against universal time. For a southward z component of the interplanetary magnetic field (IMF) one expects an antisunward drift (Coffman et al., 1977). Since the IMF data were not available for the period covered in Figure 8 we listed the Kp values. As seen here and also in other data, the drift direction is generally antisunward when Kp > 2 while strong deviations in the sunward direction are observed when Kp is very small. In the period covered by Figure 8, the most consistent antisunward convection occurs from 12 UT on 20 October to 21 UT on the next day, when Kp varies between 2 and 4. A 90° deviation is observed from midnight to 12 UT on 20 October. October 22 shows sunward convection for about 8 hours starting at 12 UT when Kp = 1. The Qanaq ionogram survey (vertical 0 trace only) for 20 October (Figure 9) reveals that the F region was disturbed until 12 UT, and the F traces show spreading and forking. After 12 UT, when the drift is consistently antisunward, the ionogram signatures are different, suggesting a fairly smooth ionosphere, even though Kp increases to 4.

4. Conclusions

The growing Digiscand 766 network makes it possible for the first time to obtain electron density profiles of the bottomside ionosphere on a global basis with good time resolution. All the data reduction is done in real time leaving only data editing and display to be done off line. It seems that this data base can provide the test bed for the ionospheric modeling efforts. A world-wide study of the ionospheric roughness and the ionospheric drift could give new inputs to the modelers. It will be important to conduct coordinated measuring campaigns to study large scale phenomena like atmospheric gravity waves.

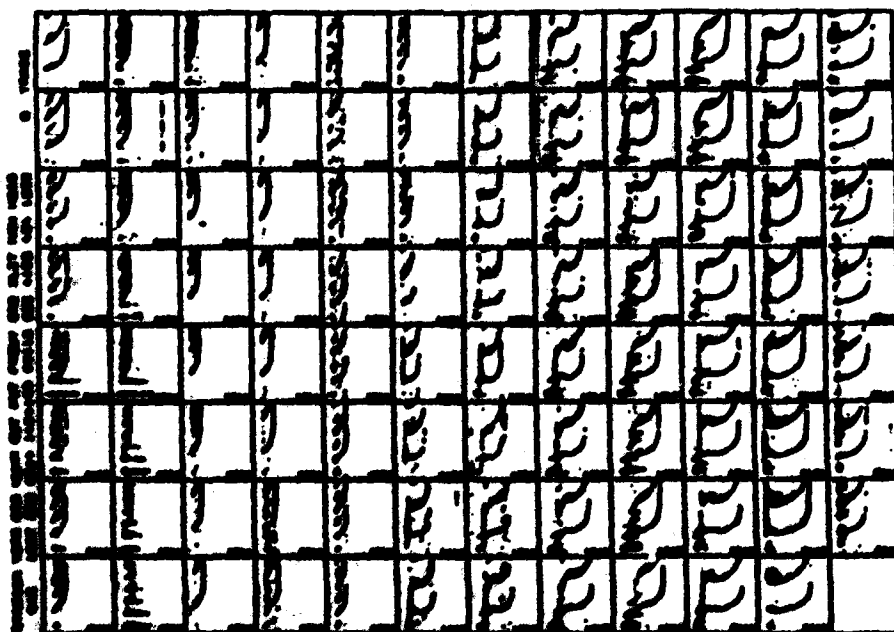
Acknowledgement

This work was in part supported by the University of Lowell and in part by the Air Force Geophysics Laboratory, Hanscom AFB, Massachusetts.



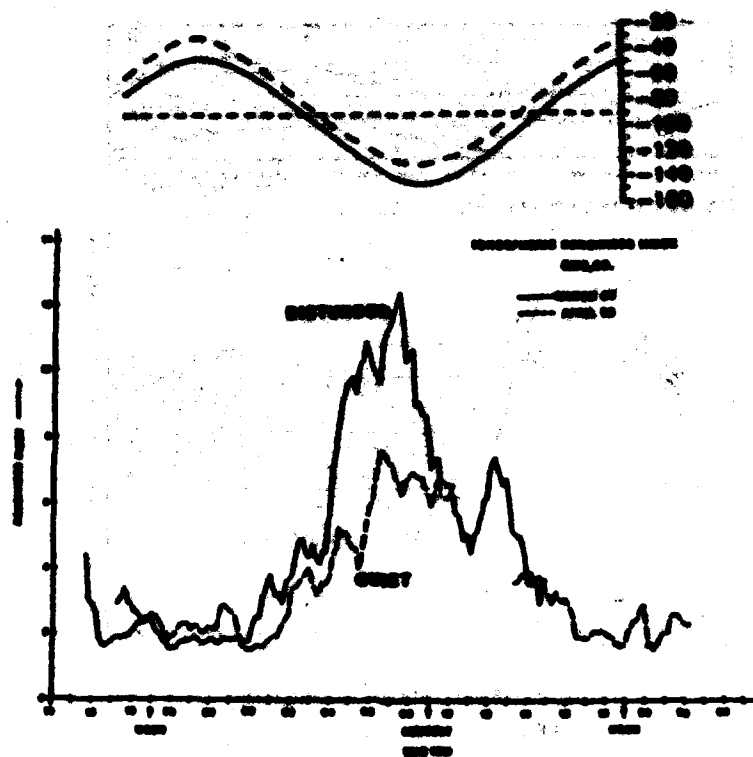
IONOSPHERIC CHARACTERISTICS
MILLSTONE, MA 20 OCT 1997

Figure 3



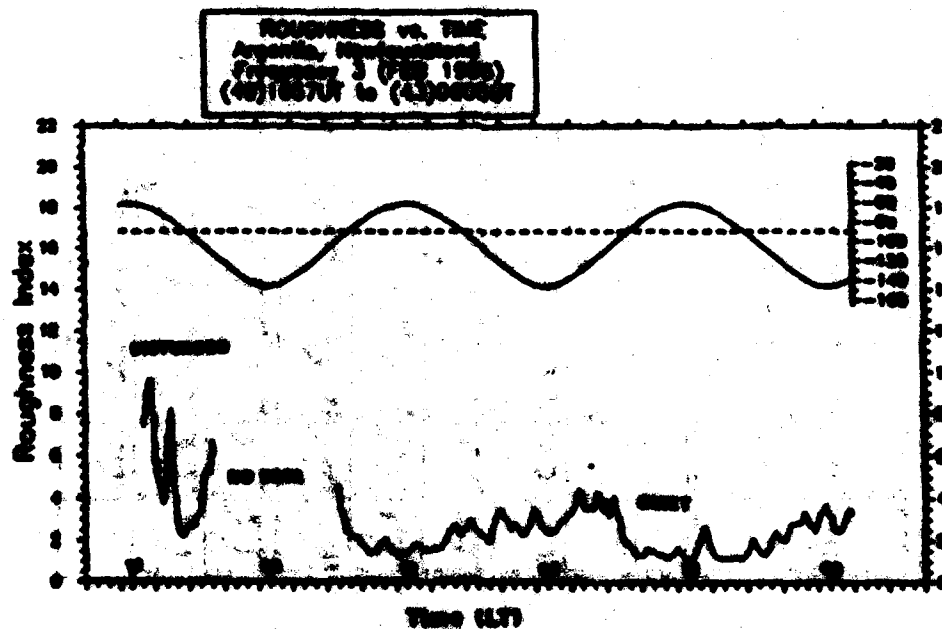
IONOGRAM SURVEY (X Trace and Oblique Signals Suppressed)
MILLSTONE, MA 20 OCT. 1997

Figure 4



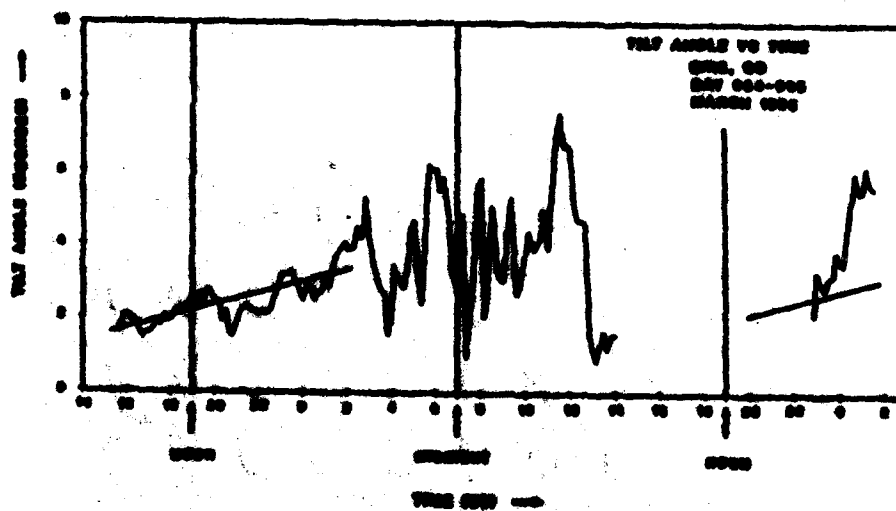
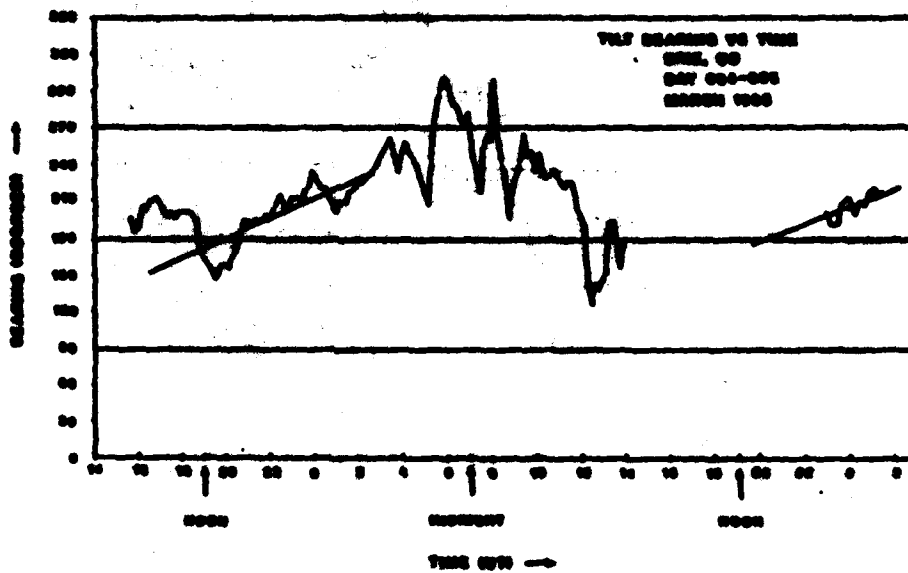
DIURNAL VARIATION OF ROUGHNESS INDEX

Figure 3



ROUGHNESS INDEX FOR DIURNAL T LATER

Figure 4



VLF ANGLE FOR REGISTRATION 9 LATER

Figure 7

1-200000
 1-200000
 1-200000

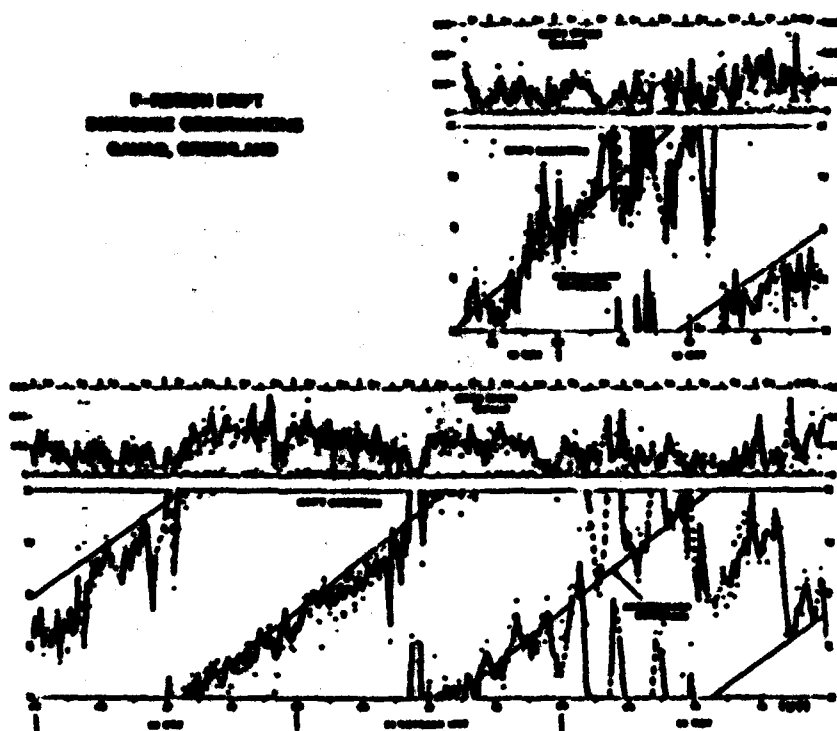
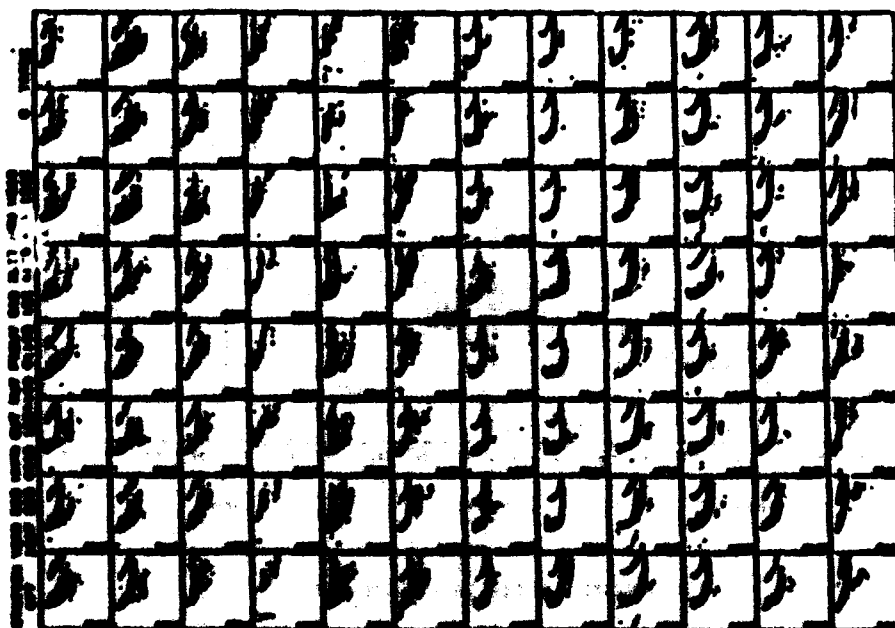


Figure 8



1-200000
 1-200000
 1-200000

Figure 9

SECRET
 REF ID: A67111

Almed, S., G. S. Sales and S. W. Rainich, "Frequency Management of a Long Range HF Communication Link US-UK (Conventional Data)," Proceedings of the IEEE MILCOM Conference, pp. 300-303, October 30-31, 1968.

Buchan, J., S. G. Schuman, H. E. Anderson, E. J. Weber and C. Dennis, "Foliar Gap Plasma Conversion Measurements and Their Relevance to the Real-Time Modeling of the High Latitude Ionosphere," Proceedings of IED 67 Symposium on the Effect of the Ionosphere on Communication, Navigation, and Surveillance Systems, May 5-7, 1967.

Dennis, C. G., "A High Frequency Radio Technique for Measuring Plasma Drifts in the Ionosphere," Scientific Report No. 6, AFOSR-78-63-0001, Hanscom AFB, Massachusetts, July 1968. unann

Gonzalez, R. S., W. T. Harvey and S. W. Rainich, "Electron Density Profiles from Automatically Sealed Digital Ionograms. The ARTIST's Valley Solution," Scientific Report No. 1, AFOSR-78-63-0001, 1968. unann

Gilbert, J. D. and S. W. Rainich, "A Comparison Between the Automatic Ionogram Sealing System 'ARTIST' and the Standard Manual Method," submitted to Radio Science for publication in 1969.

Potomac, J. A., K. Bibl and S. W. Rainich, "Direct Digital Graphics, The Display of Large Data Fields," American Laboratory, pp. 96-101, September 1972.

Rainich, S. W., "New Techniques in Ground-Based Ionospheric Sounding and Studies," Radio Science, 12, No. 3, pp. 521-541, May-June 1977.

Rainich, S. W. and George Koppa, "Automatic Circulation of Electron Density Profiles from Digital Ionograms. 1. Processing of Ionograms," Radio Science, 12, 3, pp. 477-487, May-June 1977.

Rainich, S. W., H. Almed, K. Bibl, H. Suiter, F. Gorman, J. D. Jodanis, L. Bessy, J. King and J. Gilbert, "A Transatlantic Digital HF Radio Link Experiment," Proceedings of the Ionospheric Effects Symposium, Effect of the Ionosphere on C-I Systems, Alexandria, Virginia, pp. 111-122, May 1-3, 1969.

Rainich, S. W., J. Buchan and E. J. Weber, "Digital Ionosonde Observations of the Foliar Gap / Region Conversion," Physics Scripta, 22, pp. 373-377, 1967.

REAL TIME ELECTRON DENSITY PROFILES FROM IONOSPHERES

Bodo W. Reinisch, Robert E. Garriot, Huang Xueqin* and
Law F. McPherson

*University of Lowell Center for Atmospheric Research, Lowell, MA 01854,
U.S.A.

Research Institute of Radio-wave Propagation, P.O. Box 130, Hsinchu, Taiwan,
ROC

Andersson, Australian Research Council, Parkville, Victoria, 3052, Australia

ABSTRACT

Knowledge of the three dimensional electron distribution in the earth's ionosphere is a requirement for both the radio communication engineer and the geophysicist studying the ionosphere and for investigation with the current ionosphere in terms of reflection and particle input from the sun. Global coverage with adequate spatial and temporal resolution must be provided by any data base if it is to be useful for the modeler.

At the present time, one of the best global distributions of the electron density is given by the International Reference Ionosphere (IRI-70) [1]. The IRI model is based largely on observational data obtained with ionosondes, ionospheric sounder radar, satellite and rocket. Amongst these techniques, the ionospheric observations provide the best global coverage and, in principle, the best time resolution. The disadvantages of the ground-based ionosonde technique are well known: (1) no information on the topside F region, (2) limited accuracy for the lower E-region and the valley ionization between the E and F regions, and (3) continuous evaluation of electron density profiles from the ionograms. Nevertheless, the existence of some ionosonde stations providing more or less continuous day and nighttime profiles constitutes the ionosonde network as an important contributor to the electron density data base.

As a result of advances in the electronic computer area and the micro-computer field, modern ionosondes are available today that serve the need for manual conversion of the ionogram into vertical electron density profiles. Reinisch [2] showed that modern ground-based ionosondes can supply the profiles in real time, overcoming one of the limitations of ionosondes. If complementary data from modern topside ionosondes were available we could have a very comprehensive data base. In 1970, Reinisch and Llewellyn [3] used existing Alouette topside ionogram data for the modeling of the topside F region. Today these or four modern ionosondes [4] show on existing satellites could provide automatic topside profile information on a world-wide basis. Automatic scaling techniques for topside ionograms already exist [5, 6], and vertical profiles can be represented in compact coefficient form [7]. Although such modern topside ionograms are considered for the early to mid-nineties, they are not available now, and this paper therefore concentrates on the growing network of modern ground-based ionosondes.

IONOSPHERIC NETWORK AND DATA BASE

Since the Alouette 20 [4] is the only currently available ionosonde that outputs electron density profiles in real time, we will base our discussion on this system. The Alouette 20 outputs ionograms (Figure 1) to which the vertical electron density and complementary information are directly translated [8]. It's output is the IRI-70, a 70-MHz microcomputer, to determine the virtual height traces $h'f(f)$ for the E and F regions [9] (Figure 2), and the apparent ionospheric parameters. The $h'f(f)$ traces are checked for errors (Figure 3) before the IRI-70 outputs (Figure 4) to permanent and checked (Figure 5, see [10]). The Alouette 20 height ionograms program enables in addition as will be discussed in the next section. The coefficients of the polynomial profile representation are sent to a data center (Figure 6), where data from all digital ionosonde stations are combined to obtain global ionosonde maps (Figure 7).

Figure 1 shows automatically sorted significant ionograms from a polar cap station.

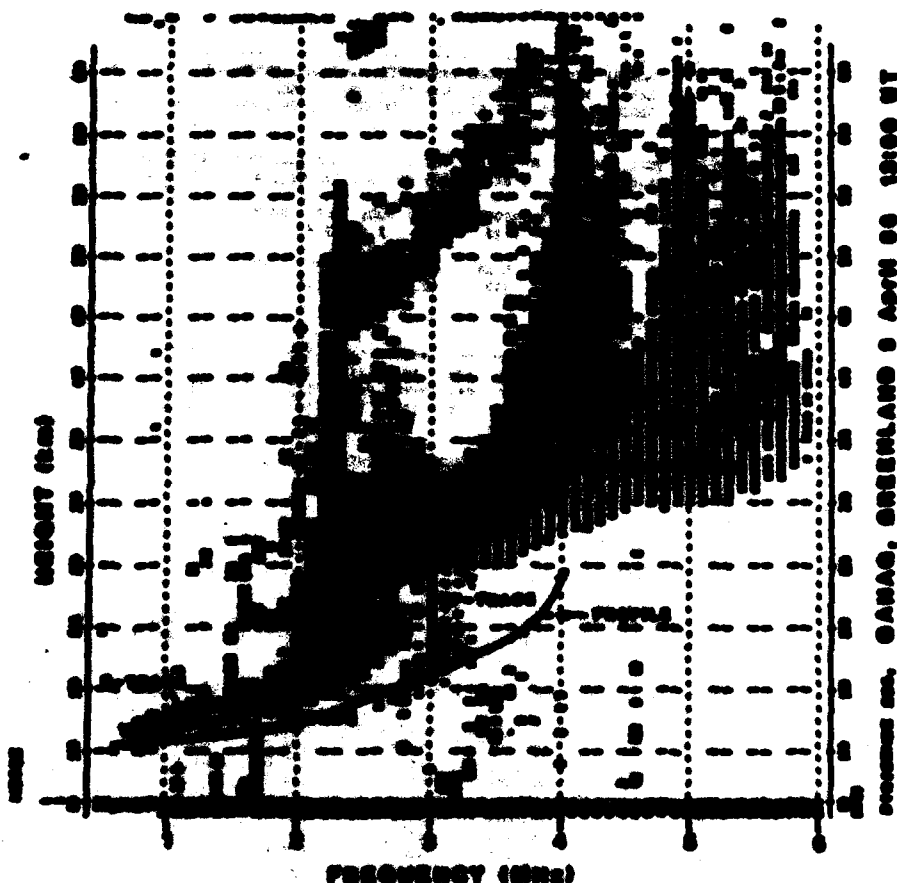


Figure 1. Polar cap ionogram

Greenland, 77.5°N, 69.5°W station. The on-line pictures of the Ques ionograms are recorded at 15:00 UT (- 14:30 local time) on 6 April 1966. The signal amplitude is in units of 5 dB and shown as numbers 1, 2, ..., if the value is positive, and as A, B, ..., if the signal is negative. Signals with conventional identification are represented as E, and other signals as F. The F-layer has identified the leading edge of the E trace (marked *) and the F trace (marked #). The electron density profile, based on the F-layer, is indicated as A. This illustrates the significant effect of the ionosphere under heavy spread conditions, typical for polar cap and auroral stations. For similar operation, the ionograms are not printed, and only the ionospheric parameters and the profile coefficients are recorded (see Table 1).

Figure 1

[illegible]

11

NOTE: The algorithm uses a set of shifted Chebyshev polynomials to approximate the true height for each intermediate layer. *1/1*

where the A_i 's are the coefficients of the polynomials, Z_0 refers to the peak height of the laser and is given by $Z_0 = \text{scat height} \cdot \sum A_i$, the Z_i 's are the shifted Chebyshev polynomials /13/, and g is

Steps 2, 3, and 4 refer to the search and cut sequences of the respective layers, and 5 is the temporary time considered. The server δ multiplying the cut answers on infinite steps at the path of the layer, where $\delta = 0$. The algorithm uses three times $(1 - 2)$ for the E layer, five times $(1 - 4)$ for the F layer step process, and three times for the F2 layer. To avoid the S.F. operation the algorithm assigns a variable which (W) also shows the E layer path (Figure 2). δ is determined by a least squares fitting procedure /14/. This simplified approach deviates from the original Hainisch-Huang method /14/, that included the search for a valley. Determination of the valley will be postponed until ARTIST provides the F layer S-data.

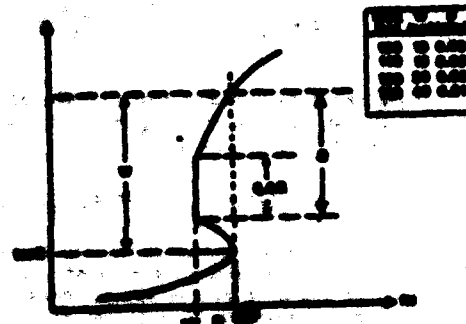
The steering height of the profile is determined by the data, also taking account of thermal dilatation and magnetic/hydrostatic disturbances. The $h'(z)$ above data (the z curve during the day, the z' curve at night) are extrapolated around $z = 0$ by assuming a parabolic profile:

where y is the height of the end condition y , Engineering the magnetic field, the corresponding

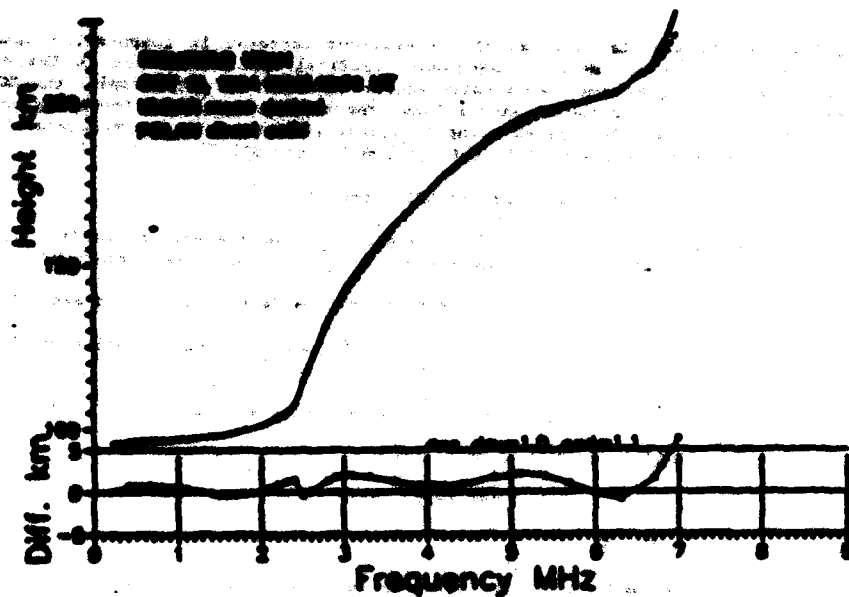
[illegible]

Technique's FIVE program is designed to 100% in the real time environment only

Page 2

**Figure 2**[illegible]

Electronic document profiles derived automatically from digital language provide a



Profile Technique Comparison

Figure 4

| Ionogram Day UT | Freq MHz | Mean Height km | Height Difference | | | | | | | |
|--------------------|-------------|----------------------|----------------------------|------------------|----------------------------|------------------|----------------------------|------------------|----------------------------|------------------|
| | | | O-wave | | | | X-wave | | | |
| | | | $\langle \Delta h \rangle$ | Δh_{max} | $\langle \Delta h \rangle$ | Δh_{max} | $\langle \Delta h \rangle$ | Δh_{max} | $\langle \Delta h \rangle$ | Δh_{max} |
| 205, 15:30 | 7.1 | 228.3 | 4.36 | 6.0 | 3.36 | 6.0 | 3.36 | 7.3 | 3.76 | 7.3 |
| 205, 16:30 | 6.6 | 217.3 | 3.60 | 13.3 | 2.62 | 13.3 | 3.32 | 13.2 | 3.31 | 13.1 |
| 205, 17:44 | 6.5 | 207.0 | 4.86 | 7.9 | 4.36 | 7.4 | 3.36 | 16.0 | 3.29 | 16.7 |
| 207, 08:30 | 3.9 | 206.0 | 2.48 | 9.6 | 2.48 | 9.6 | 0.39 | 9.3 | 4.00 | 3.6 |
| 207, 09:30 | 3.9 | 205.4 | 1.37 | 7.3 | 1.37 | 7.3 | 4.44 | 9.6 | 2.18 | 6.8 |
| 207, 10:30 | 4.6 | 202.4 | 2.56 | 3.6 | 2.52 | 3.3 | 2.39 | 7.7 | 4.66 | 7.6 |
| 207, 11:30 | 3.3 | 186.7 | 1.44 | 9.1 | 1.32 | 9.7 | 1.09 | 10.0 | 2.71 | 16.0 |
| 207, 12:00 | 6.6 | 200.7 | 2.13 | 13.3 | 2.42 | 13.0 | 1.94 | 16.3 | 1.37 | 16.4 |
| 207, 12:30 | 2.3 | 200.4 | 1.46 | 7.8 | 2.42 | 6.3 | 1.91 | 9.6 | 2.04 | 6.6 |
| 207, 13:30 | 1.3 | 200.7 | 1.32 | 13.1 | 1.37 | 13.3 | 1.16 | 13.3 | 2.16 | 11.3 |
| 207, 14:30 | 6.9 | 200.7 | 1.32 | 13.1 | 1.71 | 13.1 | 1.54 | 9.3 | 2.22 | 6.3 |
| 207, 15:30 | 6.7 | 200.1 | 2.40 | 13.7 | 1.36 | 13.7 | 1.36 | 13.6 | 1.06 | 13.6 |
| 207, 16:30 | 7.3 | 200.1 | 4.36 | 13.1 | 4.11 | 13.1 | 3.36 | 13.7 | 3.06 | 13.7 |
| 207, 17:30 | 7.4 | 200.9 | 4.36 | 13.3 | 4.36 | 13.7 | 3.36 | 13.6 | 2.96 | 13.6 |

Table 2. Mean absolute height difference for normal operational modes

Values are given for the average of single values of the ionograms. Single values of the ionograms have been used for comparison in applications in which the errors in the resulting

calculations are stopped because of the enormous decrease in computation time which such models provide. One of the most important practical applications is in the calculation of electron field strength and transmission losses at HF. For example, the GMR Supplement to Report 252 /14/. For other calculations, the propagation codes involving reflection from the E and F layers are described using an ionospheric model with parameters which depend on the routinely scaled values of f_{oE} , f_{oF} , $M(3000)F_2$ and $h'F_2$.

The model currently recommended by GMR consists of:

A parabolic E layer below its height of maximum electron density, h_{mE} , with semi-thickness y_{mE} . h_{mE} and y_{mE} are set to 110 km and 20 km respectively.

A parabolic F2 layer with height of maximum density h_{mF2} , and semi-thickness y_{mF2} .

A linear increase of electron density between h_{mE} and the point on the parabolic F2 layer where the plasma frequency is 1.7 f_{oE} .

The model parameter h_{mF2} is given by the empirical equations /14/, /17/:

$$h_{mF2} = 1400 / (M(3000)F_2 + 0.01) + 170 \quad (4)$$

$$\text{with } 0.1 \leq M(3000)F_2 \leq 1.4 + 0.005 (M(3000)F_2 - 20) / 100 \quad (5)$$

$$\text{and } 1 \leq f_{oE} / f_{oF}, \text{ or } 1.7, \quad (6)$$

whichever is the larger. $M(3000)F_2$ is the 30-MHz modified critical number.

The term 0.01 in eq. (4) is an empirical correction term which takes into account the effects of underlying ionization not allowed for in the original Shimozaki /14/ formulation. Model estimates of h_{mF2} are usually considered to be correct to within 20 to 30 km /14/. Saitoh /18/ has described an improved model which uses a cosine F2 layer shape and a more realistic E-F transition region, and has found that this model yields more accurate values of h_{mF2} than the Saitoh-Saitoh /17/ model. Saitoh gives a revised formula for h_{mF2} :

$$h_{mF2} = 1400 / (M(3000)F_2 + 0.01) + 170 \quad (7)$$

$$\text{where } 0.1 \leq M(3000)F_2 \leq 1.333 + 0.012 \quad (8)$$

$$\text{and } 1 \leq f_{oE} / f_{oF} \leq [(0.005 f_{oE}^2 + 1) / (1.005 f_{oE}^2 - 1)]^{0.5} \quad (9)$$

The value of 1 in eq. (9) is considered to exceed 1.215.

Shimozaki, Shimozaki and Tani /19/ have analyzed the differences between the F2LH and Saitoh values of h_{mF2} for the four different stations, according to the value of 1 ($= f_{oE} / f_{oF}$) and to the value of the electron loss 0.1 .

Table 3 shows that the differences change from being systematically positive for low 1 values, to being systematically negative for high 1 values. Negative differences indicate that the F2LH value is less than the Saitoh value. The average discrepancy is about -5 km, but this value is highly a function of the values of 1 and in the different ranges of 1 . In general, the high 1 values correspond to nighttime conditions. For $1 \leq 1$, the differences are in the range of -10 to -20 km.

$$\Delta h_{mF2} = h_{mF2} - h_{mF2}^{\text{Saitoh}} = -0.2 \text{ km} \quad (10)$$

From this table one can see that the differences are also large when 1 is the greatest. The overall accuracy of the Saitoh model is very dependent on such a simple model.

| Altitude meters | Percentage Distribution of Occurrences of | | | | | Total |
|--------------------|---|-------|-------|-------|-------|-------|
| | 1-10 | 11-20 | 21-30 | 31-40 | 41-50 | |
| 10-15 | 1 | 1 | 10 | 12 | 4 | |
| 15-20 | 1 | 0 | 11 | 20 | 8 | |
| 20-25 | 0 | 1 | 20 | 20 | 13 | |
| 25-30 | 0 | 0 | 14 | 17 | 8 | |
| 30-35 | 4 | 24 | 17 | 8 | 13 | |
| 35-40 | 11 | 24 | 10 | 4 | 14 | |
| 40-45 | 20 | 20 | 4 | 8 | 12 | |
| 45-50 | 25 | 0 | 3 | 1 | 9 | |
| 50-55 | 25 | 0 | 0 | 3 | 8 | |
| 55-60 | 9 | 0 | 0 | 2 | 4 | |
| 60-65 | 7 | 1 | 1 | 1 | 3 | |
| 65-70 | 1 | 1 | 1 | 1 | 1 | |
| Total | 200 | 245 | 94 | 100 | | |

Table 1. Percentage distribution of occurrences less than 30 km for all five stations, for four ranges of X .

The systematically high values of h'_{min} given by the Svalbard records at night may be due to the code's neglect of underlying ionization. The effect of this underlying ionization was originally considered to be insignificant a decade or so ago, which is indeed true in comparison with the effect of the E and F₂ layers during the day. However, the daytime records have been improved to the point where the nighttime errors are now the largest observed.

An alternative explanation may lie in the variation with altitude of the F₂ region scale height, which is not accounted for by the Svalbard model.

DATA REPRESENTATION AND ANALYSIS

Systematically long-term data have been recorded on Sita and the format suggested for inspecting the ionograms. Today, station ionograms display the ionograms on fluorescent screens in real time (Figure 1), and store the essential data in digital form on magnetic tape. Unfortunately, there is no general consensus as to what is essential. For routine operation at any station it is necessary to store the essential portions of the vertical traces as well as the essential parameters, and, since they are available, the coefficients of the electron density profile. The ionograms can be directly photographed within one hour of their recording. The Svalbard data include vertical trace data, which make 5,000 ionograms can be recorded on a standard 1000 ft tape, or a 1000 ft tape can store 10 weeks of data for quarter hourly ionograms. It is possible to write one ionogram in one hour, which would limit the number of tapes per year to three. For detailed ionogram studies all ionogram data should be retained on tape.

Graphic tape groups of the two height profiles and the automatically scaled ionograms have facilitated the analysis of all data on a very wide variety of tape. Two techniques have been developed at UCL to be equivalent with the data recorded from the Svalbard site.

The above techniques give the F₂ layer two height electron density profiles that are calculated in real time and then stored on magnetic tape. A composite of the profiles for one day is presented in Figure 2. The three dimensions, height, time and electron density, are displayed as ordinate, abscissa, and a 16 level gray scale (Opticon, /11/).

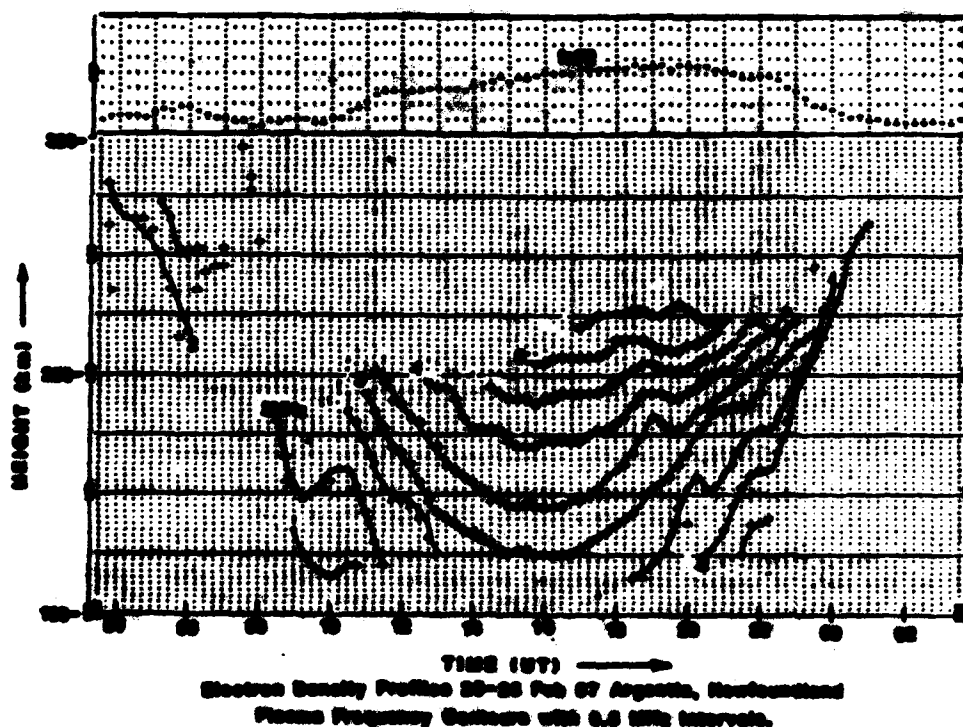


Figure 3

respectively. Ion-electron density contours result that are a function of time and height. Several features can be seen: the compression of the daytime F-layer to relatively low heights with short time variations that have a wave-like appearance and are likely associated with traveling ionospheric disturbances.

A second technique that we are finding useful for survey and study is a single sheet presentation of the day's complete, automated, ionograms. At a glance, one can easily detect events such as compression of sporadic E, sudden ionospheric disturbances, and the development of the dawn F-layer trough and the seasonal oval. The single sheet compilations make day-to-day comparisons easier than with film archival. They also enlarge dramatically the information content when compared to tables of scaled ionospheric parameters.

The examples shown here are but several of many that may prove useful for data presentation and archival. A key point is the recognition that magnetic media storage of ionospheric data enables complete, edited, and presentations which heretofore were impossible or very labor intensive. The system, however, whether in space or on the ground, continues to produce important data for understanding ionospheric phenomena and for development of more realistic global ionospheric models. Additionally, the utility of these data is not limited by the storage media, and open new opportunities for tailored data presentation, archival and analysis consistent with the needs of a specific research study.

REFERENCES

1. K. Bauer, IEEE Trans. AP-29, World Space Center A (S.T.P.), Boulder, CO, USA (1981).
2. B. W. Reinisch, Radio Sci. 21, no. 3, 331-341 (1986).
3. B. B. Bost and S. K. Llewellyn, IEEE Trans. AP-28, Melbourne, FL, USA (1980).
4. H. E. Mathwick, D. E. Ashert, A. F. Horan, R. Sibl, B. W. Reinisch and B. Lewis, in Proceedings of the 1981 J. Goodman, Alexandria, Va., 634-643 (1981).
5. B. W. Reinisch and X. Huang, Radio Sci. 17, no. 4, 421-434 (1982).
6. S. Igi and K. Akiyo, Journal of the Radio Research Laboratory 33, no. 4, 169-183 (1986).
7. X. Huang and B. W. Reinisch, Radio Sci. 17, no. 4, 637-644 (1982).
8. B. W. Reinisch, Science 236, in IEEE Bulletin 448.
9. R. Sibl and B. W. Reinisch, Radio Sci. 13, no. 3, 319-330 (1978).
10. B. W. Reinisch and X. Huang, Radio Sci. 18, no. 4, 477-492 (1983).
11. L. F. McManus, Scientific Summary No. 1, AFRL-TR-86-0098, WAFB-432/OMR (1986). ADA171320
12. J. E. Tichard, IEEE Trans. AP-29, World Space Center A (S.T.P.), Boulder, CO (1981).
13. H. A. Snyder, Shannon Method in Electrical Communication, Prentice Hall, New Jersey (1964).
14. B. W. Reinisch, R. Sibl, C. G. Davis, R. E. Gonsky, D. F. Kitzinger, S. W. Li, G. S. Sales and S.-H. Tseng, Final Report, AFRL-TR-87-0066, (1987). ADA192270
15. L. F. McManus, IEEE Trans. AP-27, 343-348 (1979).
16. ITU, Summary of Report 33, International Radio Consultative Committee, International Telecommunication Union, Geneva, Switzerland (1980).
17. F. A. Bradley and J. R. Sweeney, J. Atmos. Terr. Phys. 33, 2131-2146 (1973).
18. T. Shimozaki, J. Radio Res. Lab., Japan, 2(7), 56-97 (1985).
19. J. R. Sweeney, J. Atmos. Terr. Phys. 45, 629-646 (1983).
20. L. F. McManus, B. W. Reinisch and J. S. Tseng, Adv. in Space Research (1987).
21. J. Focuss, R. Sibl and B. W. Reinisch, American Laboratory, 95-101, September 1973.

ACKNOWLEDGMENT

The work of the University of Lowell authors was in part supported by the Air Force Geophysics Laboratory, Hanscom Air Force Base, Massachusetts.

LAY-FUNCTIONS FOR F2 PROFILES

L. Bazy*, R. R. Gurnee** and B. W. Reinisch**

*Université Catholique de Louvain, S-1348 Louvain-la-Neuve, Belgium

**University of Lowell Center for Atmospheric Research, Lowell MA 01854,
 U.S.A.

INTRODUCTION

Recent ionosonde /1/ calculate the vertical electron density profiles in real time providing a good data base for the global modeling of the ionospheric electron density distribution. The Digisonde 250 outputs the profiles in form of coefficients for a polynomial representation /2/ for each of the layers. When Oliver published their results, Reinisch and Huang /3/ mentioned the possibility of substituting LAY functions for the polynomial profile representations. In this paper we study the starting of LAY functions profiles obtained in real time by Digisonde at Antigua, Newfoundland (47°N, 54°W), Richfield, Utah (39°N, 112°W) and Natal, Brazil (5.7°S, 35°W). We use the technique proposed in /4/ to determine the LAY parameters f_oF_2 and $h'F_2$. Because of the efficiency this algorithm lends itself to real time processing.

FITTING OF LAY FUNCTIONS AND IMPLEMENTATION

The representation of the electron density profile of the F2 layer by a single LAY function is discussed. The LAY function used for this purpose has described in Reference 4. The advantage of the LAY function fit of the profile is that in general the entire F2 profile is well represented by one LAY function, defined by only four parameters f_oF_2 (critical frequency), $h'F_2$ (peak height), $h'F_2$ (scale parameter) and $h'F_2$ (scale parameter) /4/. Other methods like the third order polynomial representation requires five coefficients plus the beginning and ending frequency of the layer. Titcheridge's FOLAN wave height analysis program /5/, in its polynomial mode (P), uses six coefficients $a_0, a_1, a_2, a_3, a_4, a_5$ plus the starting frequency and height; in the FOLAN polynomial mode used in the Digisonde (a 4th order polynomial), 11 parameters are needed to represent the F2 profile.

LAY function fitting was performed for some three thousand electron density height profiles which were calculated from ionograms with the FOLAN method using a fourth order polynomial expansion of the F2 profile. The form of the LAY function always ensures a good fit on the layer path, but it must be checked how far down in frequency the fit is acceptable. We defined error thresholds of 1 m, 2 m and 10 m to determine the lower frequency limit of the fit. The 1 m threshold resulted in too narrow frequency intervals for which the fit is acceptable, and 10 m appears too coarse a measure. With a 2 m error, the LAY functions can describe almost the entire F2 region, so we decided to select the 2 m threshold for further analysis.

Our LAY analysis program computes and records the average absolute error per point in m, together with the number of frequency points and the threshold frequency f_{min} . The values of f_oF_2 , $h'F_2$ (when present), $h'F_2$, and the inflection point of the F2 profile are saved to study the range of the LAY fits. From the parameters the ratios $h'F_2/h'F_2$ and $(h'F_2 - h'F_2)/h'F_2$ are calculated and stored. Since the profiles are available, we also calculate the factor C from $h'F_2(0.5) - C h'F_2$ (about $h'F_2(0.5)$) to the height where the electron density is $N = 0.5 N_{max}$. The C factors found for the profiles are compared with the value $C = 0.5$ suggested by Chapman /6/.

Figure 1 is an example of the LAY function fits to a profile from Richfield, Utah, October 11, 1976 at 20:00 UT (23:00 LT). Here the particular LAY function plotted is for fitting points at $f_1 = 0.90500$ and $f_2 = 0.90500$ and is shown along with the profile.

*also Institut d'Astronomie Spatiale, S-1348, Louvain-la-Neuve, Belgium

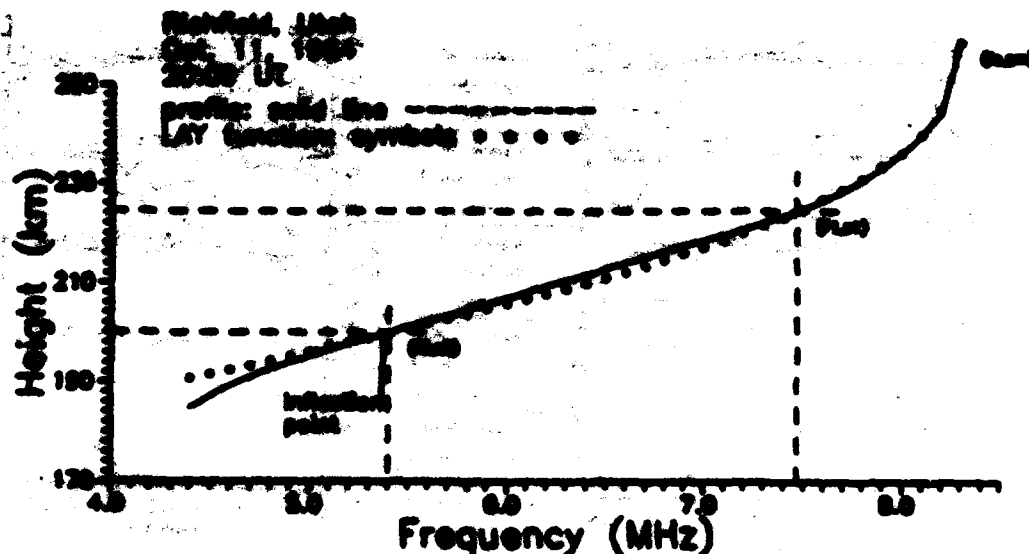


Figure 1. Fitting LAY function profile. The three selected points were (6.3 MHz, 205 km), (7.9 MHz, 224 km), and (5.4 MHz, 200 km). The LAY function approximates the F2 profile to frequencies well below the inflection point. SoF1 for this ionogram is 4.3 MHz.

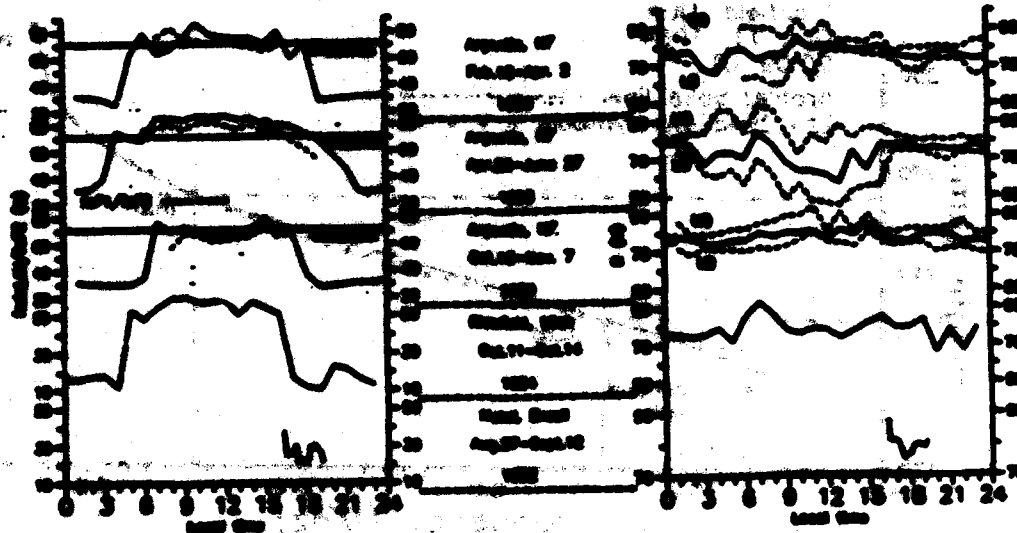
This fit has an average absolute error per point of 1.05 km with a 3 km maximum error, and agrees with the profile. The LAY parameters for this F2 profile are $h'X = 197$ km and $h'Y = 20.5$ km.

SCOPE OF VALIDITY OF THE FIT

Our studies show that apart of the time the LAY functions, with 3 km maximum error, represent the entire F2 layer down to $f = f_{min}$ or SoF1 during the day, and to the first cooled ionogram frequency during the night. The solid lines in Figure 2 represent the median values for Argentina; dashed lines are those of the tests SoF1/SoF2. For Argentina, we analyzed profiles done for February/March, May/June and October/November 1966 (the upper three curves in Figure 2). The dashed lines represent the median SoF1/SoF2 during daytime when the F1 layer exists. The Argentine data show SoF1 to be within 7% of SoF2, i.e., not more than about 300 km above SoF2. Without an F1 layer, SoF1 merges down to the lower F region. The horizontal lines at 70.7% for the Argentine curves indicate the level where the electron density N is half the maximum density of the layer.

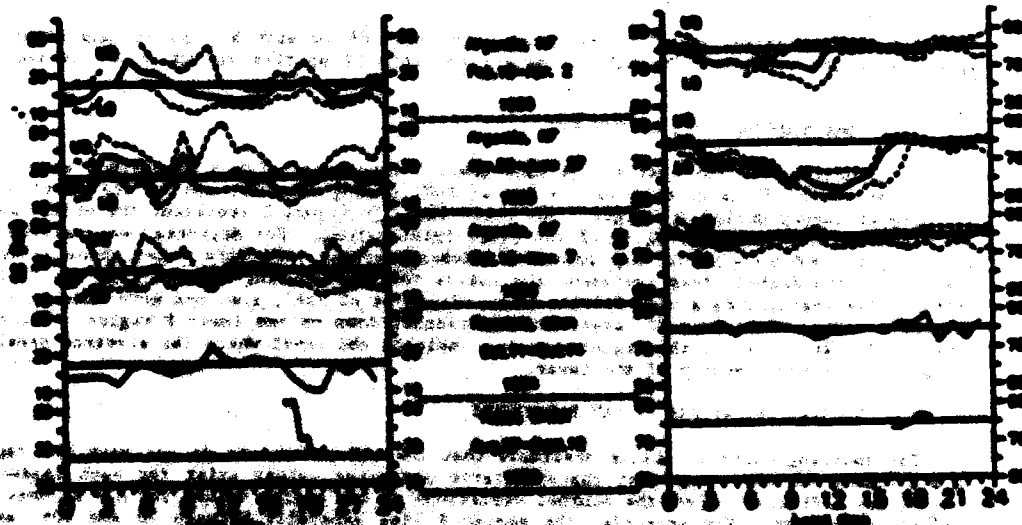
SEASONAL VARIATIONS OF LAY PARAMETERS

For modeling purposes, it is desirable that the LAY parameters do not vary too rapidly as a function of time, and that characteristic parameter values exist for each season and time of day. Figure 3 shows the seasonal variations of the median values for $h'X = h'_{min}$, expressed in percent. For Argentina, the median $h'X$ lies generally between 70 and 80%, except during summer in winter, when it dips down to 60%. The relatively large data gap for



THE UNIVERSITY OF CHICAGO PRESS

ALL INFORMATION CONTAINED HEREIN IS UNCLASSIFIED
DATE 11-14-2013 BY 60322 UCBAW



SECRET

THE UNITED STATES OF AMERICA

Argente allowed to determine the spread in h' by calculating the upper and lower quartiles, called h'_u and h'_l respectively. It is interesting to see, that for periods of small diurnal variation the data spread is also small.

The relatively large h' variations for Midfield are probably the result of the small data sample (only four days). For the equatorial station Natal, the available median h' values all lie between 75 and 80.

The median scale heights H' are generally confined to values between 25 to 210 km, at least for Argente and Midfield. The spread in H' values for Argente, as indicated by the upper and lower quartiles, is at times considerable making it difficult to select a suitable H' for modeling purposes. The equatorial data for Natal (high summer month) show a very different behavior, at least during the three hour period from 1400 to 1900 LT. H' decreases rapidly from 60 to 20 km. It would be necessary to study a larger equatorial data set to test the diurnal variation of H' at the equator.

Since all the data were available in the computer, we also calculated the Gulyarov G factor G_1 . The median values for the three stations discussed for the LFF fittings are shown in Figure 5. For Natal, the G -value is close to 50% on all three stations. However, substantial deviations exist in early spring and summer at Argente, when during daytime the median value drops below 50%. Of course, this is the effect of the F1 layer. In summer G_1 is consistently larger than 0.707 h'_{F1} , i.e. $G_1(h'_{F1}) > 0.5 h'_{F1}$ during the day (Figure 2), and the F2 layer shape factor G is ill defined.

CONCLUSIONS

The F2 layer profiles can be expressed in terms of LFF functions with parameters h'_{F2}/h_{min} and h' that have a fairly small diurnal variation in their median values. Our studies could be expanded to express the entire E-F1-F2 profile as a linear combination of LFF functions, and investigate whether the LFF parameters h'_{F2}/h_{min} and h' still maintain a systematic behavior.

REFERENCES

1. S. W. Heinrich, New Techniques in Ground-Based Ionospheric Sounding and Studies, *Radio Sci.* 21, no. 331-341 (1986).
2. S. W. Heinrich, R. E. Canache, E. Sany and L. F. Hoffmann, Real Time Electron Density Profiles from Ionograms, *This Issue* (1987).
3. S. W. Heinrich and Eddy Sany, Automatic Calculation of Electron Density Profiles from Digital Ionograms. 3. Processing of Ionograms, *Radio Sci.* 18, no. 477-492 (1983).
4. L. Sany, The Determination of LFF-Parameters for a Given Profile, *Adv. in Space Sci.* Vol. 7, No. 6, p. 30 (1987).
5. J. E. Titheridge, Ionogram Analysis with the Generalized Program POLAR, *Space Sci. 21*, World Space Center & (S.T.F.), Boulder, CO (1986).
6. T. L. Gulyarov, Implementation of a New Characteristic Parameter into the IRI Sub-Pack Electron Density Profile, *Adv. Space Sci.* 2, No. 20, 191-194 (1983).

ACKNOWLEDGMENT

The work of the University of Lowell authors was in part supported by the Air Force Geophysics Laboratory, Hanscom Air Force Base, Massachusetts.

